An Integrity and Quality Control Procedure for use in Multi Sensor Integration

P.J.G. Teunissen
Delft University of Technology, The Netherlands

Proceedings of the 3rd International Technical Meeting of the Satellite Division of the Institute of Navigation (ION GPS 1990), Colorado Spring, CO, September 1990, pp. 513-522.

ABSTRACT: Real-time estimation of parameters in dynamic systems becomes increasingly important in the field of high precision navigation. The real-time estimation inevitably requires real-time integrity monitoring of the models underlying the navigation system. This paper presents a real-time recursive detection, identification, and adaptation (DIA) procedure for use in integrated navigation systems. It is based on the concept of multi-sensor integration and makes use of the redundancy information stemming from both the measurement model and dynamic model. The tests proposed are optimal in the uniformly-most-powerful-invariant sense. Their inverted power function is used to introduce the concept of minimal detectable biases (MDB). The MDB is a diagnostic tool for inferring the detectability of particular model errors. It can be used for the design of a navigation filter that allows for a sufficient control on the presence of bias.

CONTENTS:

1. Introduction
2. Filtering and Testing
3. Detection
   3.1. Local Detection
   3.2. Global Detection
4. Identification
   4.1. Local Identification
      4.1.1. Single model error
      4.1.2. Multiple model errors
   4.2. Global Identification
5. Adaptation
6. The Minimal Detectable Bias (MDB)
7. References

1. INTRODUCTION

Autonomous navigation system integrity monitoring using redundant information becomes increasingly important in the field of high precision integrated navigation. It is well known that the minimum mean squared error navigation filter produces optimal estimators with well defined statistical properties. The estimators are unbiased and they have minimum variance within the class of linear(ized) unbiased estimators. The quality of the estimators is, however, only guaranteed as long as the assumptions underlying the mathematical model hold. Misspecifications in the model due to, e.g., outliers, sensor failures or state vector biases, will invalidate the results of filtering and thus also any conclusion based on them. It is therefore of importance to have an autonomous means of monitoring the integrity of the assumed mathematical model.

The present paper develops a general procedure for the real-time validation of both the measurement model and dynamic model of an integrated navigation system. The subject of system integrity monitoring has been studied extensively in the last few decades for a variety of applications in the fields of geodesy, surveying, photogrammetry, and navigation. System integrity techniques have been studied in deformation analysis for the detection and identification of possibly conflicting hypothesized geophysical models, e.g. [1, 2]. In surveying and photogrammetry, integrity monitoring techniques have been developed for the detection and identification of outliers in geodetic networks, e.g., [3-7]. More recently, integrity monitoring techniques have been proposed for navigation applications based on inertial navigation systems, GPS, and radio positioning systems such as Omega and Loran-C, e.g., [8-14]. The theory presented in this paper is applicable to dynamic systems that can be formulated in the state-space formalism and can be seen as an extension of the static *quality control theory* as developed at the Delft Geodetic Computing Centre [1-7]. Our testing procedure is recursive and can be computed in real-time through a scheme that closely parallels the standard navigation filter.

The contents of the paper are as follows. In the second section we briefly discuss the model underlying linear(ized) dynamic systems and introduce the standard recursive navigation filter. In this section we also introduce a test statistic T that is optimal in the uniformly most-powerful-invariant sense for testing for the presence of biases in the predicted residuals. All test statistics presented in the paper for detection and identification can

be seen as special cases of T . Since it is quite natural for most navigation applications to have a dynamic model available, the redundancy information stemming from the dynamic model has been incorporated in T . For those cases where a dynamic model is absent, the corresponding test statistics can be obtained analytically from T , by simply taking the limit of T as the variance matrix of the predicted state grows to infinity. In this way, the integrity monitoring techniques for static systems can be seen to be special cases of those developed for dynamic systems. This is pointed out in the paper for some integrity monitoring techniques that have recently been proposed for GPS.

Our recursive DIA-procedure consists of three steps: 1. *Detection*, 2. *Identification*, and 3. *Adaption*. Detection is discussed in the third section. The objective of detection is to test the overall validity of the mathematical model. For practical reasons a distinction is made between local validity and global validity of the model. In this way one can accommodate the detection of model errors that have either a local (e.g., outliers) or more global (e.g., soft failures) character.

In the fourth section, the identification of model errors is discussed. This step in the procedure consists of a search among all candidate alternative hypotheses for the most likely model error and most likely starting time, *l.* A distinction is made between single and multiple model errors. For the case of multiple model errors, a backward recursion method is discussed that enables one to identify the *b*-number of most likely model errors. As with detection, we distinguish between local and global identification. The test statistic for global identification is equipped with a moving window, to bound both the computational burden and delay in time of identification. The moving window may be of finite size or fading as time proceeds.

Adaptation is discussed next. Adaptation follows identification and is needed to eliminate the presence of biases in the filtered state of the integrated navigation system. Because of the possible delay in time of identification, adaptation is, strictly speaking, needed for the complete time interval from time *l* to the time of detection *k.* This, however, as a consequence would involve smoothing and may therefore be too heavy a computational burden. It is therefore proposed to simply adapt the state from time *k* onwards. The approximations involved in this simple approach can be considered negligible if the build up of model errors is still too small to be detected with a powerful enough test statistic.

The material of the final section is based on the concept of the power of a statistical test. Since one is generally in practical applications less interested in the power probability than in the bias that generated it, it is proposed in this section to use the inverted power function. In this way boundary values of the biases can be generated that are detectable with a certain prefixed reference probability. These biases are termed minimal detectable biases (MDB). The MDBs provide a means of having bias estimates available at the designing stage of the navigation filter. Their impact on the state vector or functions thereof can then be used to set acceptance criteria for the sizes of the model errors that should be detected with the test statistics at a fixed probability.

2. FILTERING AND TESTING

In this section we briefly review the mathematical model of the discrete time linear(ized) dynamic system under the null hypothesis, H_0, the corresponding recursive filtering equations that define the optimal estimators of the system state, and the uniformly-most-powerful-invariant test statistic for testing H_0 against an alternative hypothesis, H_a.

The *dynamics* of the system are modeled by the equation

$$x_{k+1} = \Phi_{k+1,k} x_k + d_k \quad , \quad k = 0,1,\ldots \tag{1}$$

where x_k is the *n*-dimensional state vector at time k, $\Phi_{k+1,k}$ is the known *n*-by-*n* transition matrix, and d_k is the process noise, assumed to be Gaussian distributed with mean zero and known covariance matrix

$$\mathrm{E}\{d_k d_l^T\} = Q_k \delta_{kl}. \tag{2}$$

where $\mathrm{E}\{.\}$ denotes the mathematical expectation operator and δ_{kl} denotes the Kronecker symbol. The initial state x_0 is also Gaussian distributed with known mean, $\hat{x}_{0|0}$, and known variance matrix, $P_{0|0}$, independent of d_k The *observables* of the system are modeled by the equation

$$y_k = A_k x_k + e_k \quad , \quad k = 1,2,\ldots \tag{3}$$

where A_k is a known m_k-by-*n* design matrix and the measurement noise, e_k , independent of d_l and x_0 , is Gaussian distributed with mean zero and known covariance matrix

$$\mathrm{E}\{e_k e_l^T\} = R_k \delta_{kl}. \tag{4}$$

Based on the above model, the optimal recursive prediction and filtering equations for the state estimates read

$$\begin{aligned} \hat{x}_{k|k\text{-}1} &= \Phi_{k,k\text{-}1} \hat{x}_{k|k\text{-}1} \\ \hat{x}_{k|k} &= \hat{x}_{k|k-1} + K_k (y_k - A_k \hat{x}_{k|k-1}) \end{aligned} \tag{5}$$

with corresponding variance matrices

$$P_{k|k-1} = \Phi_{k,k-1} P_{k-1|k-1} \Phi_{k,k-1}^T + Q_k$$
$$P_{k|k} = [I - K_k A_k] P_{k|k-1} \quad (6)$$

where

$$K_k = P_{k|k-1} A_k^T [R_k + A_k P_{k|k-1} A_k^T]^{-1}$$

is the so-called Kalman gain matrix

The above filter produces optimal estimators of the state vector with well defined statistical properties. The state estimators are unbiased, are Gaussian distributed, and have minimum variance within the class of linear unbiased estimators. It is important to realize, however, that optimality is only guaranteed as long as the assumptions underlying the mathematical model hold. Misspecifications in the model will invalidate the results of estimation and thus also any conclusion based on them, It is therefore of importance to have ways to verify the validity of the working hypothesis, H_0.

An important role in the process of model testing is played by the *predicted residual.* The predicted residual is defined as the difference between the actual system output and the predicted output based on the predicted state:

$$\upsilon_k = y_k - A_k \hat{x}_{k|k-1} \quad (7)$$

Under the working hypothesis, H_0, the predicted residual is Gaussian distributed with mean zero and covariance matrix

$$\mathrm{E}\{\upsilon_k \upsilon_l^T\} = Q_{\upsilon_k} \delta_{kl} \quad (8)$$

where

$$Q_{\upsilon_k} = [R_k + A_k P_{k|k-1} A_k^T].$$

This knowledge of the distribution of the predicted residual under H_0 enables us to test the validity of the assumed mathematical model.

The following two hypotheses are considered:

$$H_0 : \upsilon \sim \mathrm{N}(0, Q_\upsilon) \text{ and } H_a : \upsilon \sim \mathrm{N}(\nabla\upsilon, Q_\upsilon), \quad (9)$$

with the vector of predicted residuals defined as

$$\upsilon = (\upsilon_1^T, \upsilon_2^T, ..., \upsilon_k^T)^T. \quad (10)$$

It will be assumed that the $\left(\sum_{i=1}^k m_i\right)$-vector $\nabla\upsilon$, can be parametrized as

$$\nabla\upsilon = C_\upsilon \nabla, \quad (11)$$

where C_υ is a $\left(\sum_{i=1}^k m_i\right)$-by-$b$ matrix and ∇ is a vector of dimension b. The matrix C_υ is assumed to be known and of full rank b, and the vector ∇ is assumed to be unknown. The appropriate test statistic for testing H_0 against H_a then reads [15]:

$$\boxed{T = \upsilon^T Q_\upsilon^{-1} C_\upsilon [C_\upsilon^T Q_\upsilon^{-1} C_\upsilon]^{-1} C_\upsilon^T Q_\upsilon^{-1} \upsilon} \quad (12)$$

This expression may be written in *geometric* terms as

$$T = \| P_{C_\upsilon} \upsilon \|^2, \quad (13)$$

Where P_{C_υ} is the orthogonal projector that projects orthogonally onto the range space of C_υ, and $\|.\|$ is the norm defined by the metric of Q_υ^{-1}. Equation (13) shows that the test statistic T can be interpreted geometrically as the square of the length of the vector that follows from projecting orthogonally onto the range space of C_υ. This is shown in Figure 1.

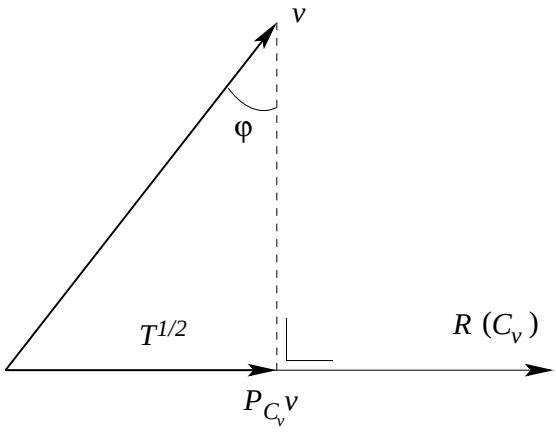

Fig. 1—Geometry of test statistic T.

The test statistic T is distributed under H_0 and H_a as

$$H_0 : T \sim \chi^2(b, 0) \text{ and } H_a : T \sim \chi^2(b, \lambda) \quad (14)$$

with non-centrality parameter

$$\lambda = \nabla^T C_\upsilon^T Q_\upsilon^{-1} C_\upsilon \nabla. \quad (15)$$

The *uniformly-most-powerful-invariant* (UMPI) test of size α is now as follows: Reject H_0 in favor of H_a if and only if

$$T \geq \chi_\alpha^2(b, 0), \quad (16)$$

where $\chi_\alpha^2(b, 0)$ is the upper α probability point of the central χ^2-distribution with b degrees of freedom. Using

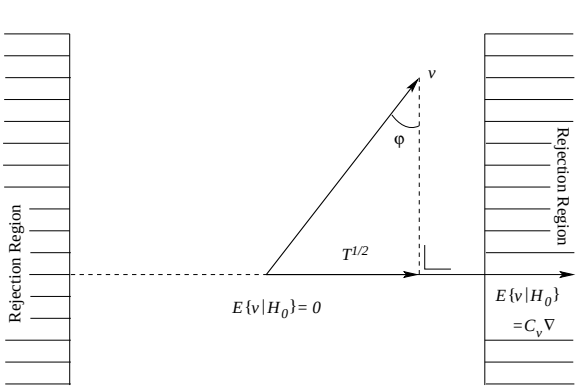

Fig. 2—Rejection region $T \geq \chi^2_\alpha(b,0)$

(16), the corresponding *rejection region* is shown in Figure 2.

At this point it is important to recognize that the above test is based on the assumption that the complete variance matrix of υ is known. For many positioning, location, and navigation applications this assumption can realistically be made. However, different test statistics are needed in case Q_υ is unknown or only partially known. For instance, the test statistic T of (12) has to be replaced by the test statistic

$$\sin^2\varphi = \frac{\upsilon^T Q_\upsilon^{-1} C_\upsilon [C_\upsilon^T Q_\upsilon^{-1} C_\upsilon]^{-1} C_\upsilon^T Q_\upsilon^{-1} \upsilon}{\upsilon^T Q_\upsilon^{-1} \upsilon}, \qquad (17)$$

if Q_υ is known up to an unknown scale factor [5, 15]. The test statistic $\sin^2\varphi$ is distributed under H_0 and H_a as

$$\begin{cases} H_0 : \sin^2\varphi \sim \mathrm{B}(b, \sum_{i=1}^{k} m_i, 0) \\ H_\mathrm{a} : \sin^2\varphi \sim \mathrm{B}(b, \sum_{i=1}^{k} m_i, \lambda), \end{cases} \qquad (18)$$

where $\mathrm{B}(f_1, f_2, \lambda)$ is the Beta-distribution with f_1, f_2 degrees of freedom and noncentrality parameter λ. The corresponding test reads therefore: Reject H_o in favor of H_a if and only if

$$\sin^2\varphi \geq \mathrm{B}_\alpha(b, \sum_{i=1}^{k} m_i, 0). \qquad (19)$$

The corresponding *rejection region* with this test is shown in Figure 3.

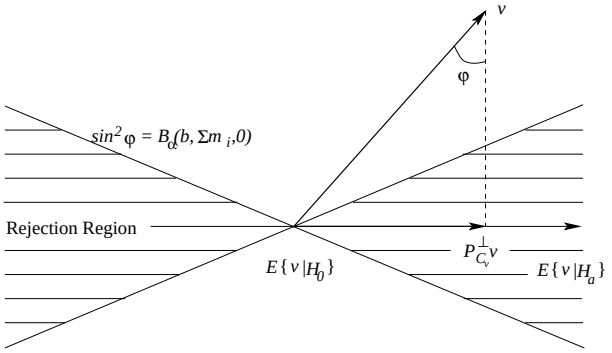

Fig. 3—Rejection region $\sin^2\varphi \geq \mathrm{B}_\alpha(b, \sum_{i=1}^{k} m_i, 0)$

In this paper we will assume that the variance matrix Q_υ is known. The above UMPI-test statistic T is therefore taken as the basis of our testing procedure for use in integrated navigation systems. It is possible, however, to generalize the theory presented in this paper for the case when Q_υ is unknown or only partially known. Our testing procedure for the real-time validation of integrated navigation systems consists of the following three steps:

1. *Detection:* An overall model test is performed to diagnose whether an unspecified model error has occurred.
2. *Identification:* After detection of a model error, identification of the potential source of the model error is needed. This implies a search among the candidate hypotheses for the most likely alternative hypothesis and their most likely time of occurrence.
3. *Adaptation:* After identification of an alternative hypothesis, adaptation of the recursive navigation filter is needed to eliminate the presence of state vector biases.

These three steps will now be discussed in more detail in the sections following.

3. DETECTION

The objective of the detection step is to test the *overall validity* of the mathematical model, H_o. For practical reasons, a distinction is made between local validity and global validity of the model. This distinction is introduced in order to have better detection and separation capabilities for model errors that have either a local or a more global character.

3.1 Local Detection

Assume that no invalidation of the model has taken place prior to the present time of testing, *k*. This implies

that attention can be restricted to the following two *local* hypotheses,

$$H_0^k : \upsilon_k \sim \mathrm{N}(0, Q_{\upsilon_k}) \text{ vs } H_a^k : \upsilon_k \sim \mathrm{N}(C_{\upsilon_k}\nabla, Q_{\upsilon_k}) \quad (20)$$

In order to test the *overall* validity of the local hypothesis H_0^k, the mean $\nabla\upsilon_k = C_{\upsilon_k}\nabla$ of υ_k under H_a^k should remain completely unspecified. This implies mathematically that the matrix C_{υ_k} should be chosen as a square and regular matrix. By restricting T of (12) to time *k,* the invertible matrix C_{υ_k} gets eliminated and the appropriate UMPI-test statistic for local detection follows as

$$T^k = \upsilon_k^T Q_{\upsilon_k}^{-1} \upsilon_k . \quad (21)$$

Note that the computation of T^k is straight forward since both υ_k and Q_{υ_k} are readily available from the navigation filter at time *k.* Since the mean of T^k under H_0^k equals the number of observables at time *k, m_k,* the dependency of the mean of T^k under H_0^k on the possibly time varying number of observables can be eliminated by normalizing (21) as

$$\boxed{T_{LOM}^k = T^k / m_k} \quad (22)$$

This UMPI-test statistic is now used to perform a local overall model test for *detecting* unspecified model errors in the local null hypothesis, H_0^k. The *local overall model* (LOM) test reads therefore as follows: An unspecified local model error is considered present at time *k* if and only if

$$T_{LOM}^k \geq F_\alpha(m_k, \infty, 0), \quad (23)$$

where $F_\alpha(m_k, \infty, 0)$ is the upper α probability point of the central *F*-distribution with m_k, ∞ degrees of freedom. The rejection region of the LOM-test is shown in Figure 4.

It will be clear that the above test statistic, T_{LOM}^k, is based on information stemming from both the measurement model and dynamic model. In fact it is a suitably weighted quadratic sum of the differences between the actual observables and their one-step predictions based on the dynamic model. In order to show how T_{LOM}^k simplifies in the case of absence of the dynamic model, we consider what happens when the limit $P_{k|k-1} \to \infty$ is taken. With the expression $Q_{\upsilon_k} = [R_k + A_k P_{k|k-1} A_k^T]$ and the identity $Q_{\upsilon_k}^{-1}\upsilon_k = R_k^{-1}\hat{e}_k$, where $\hat{e}_k = y_k - A_k\hat{x}_{k|k}$ is the *least-squares* residual of y_k, we have

$$\upsilon_k^T Q_{\upsilon_k}^{-1}\upsilon_k = \hat{e}_k^T R_k^{-1}\hat{e}_k + \hat{e}_k^T R_k^{-1} A_k P_{k|k-1} A_k^T R_k^{-1}\hat{e}_k .$$

With the least-squares orthogonality $A_k^T R^{-1}\hat{e}_k = 0$, if $P_{k|k-1} \to \infty$, it follows that

$$\boxed{\lim_{P_{k|k-1}\to\infty} \upsilon_k^T Q_{\upsilon_k}^{-1}\upsilon_k = \hat{e}_k^T R_k^{-1}\hat{e}_k} \quad (24)$$

This shows that in case of absence of the dynamic model the appropriate LOM-test statistic reads: $T_{LOM}^k = \hat{e}_k^T R_k^{-1}\hat{e}_k / (m_k - n)$. For $R_k = \sigma_k^2 \mathrm{I}_{m_k}$, it simplifies to $T_{LOM}^k = \hat{e}_k^T\hat{e}_k / [\sigma_k^2 (m_k - n)]$. This is the detector proposed in [8] and [9] for the autonomous navigation system and GPS integrity monitoring.

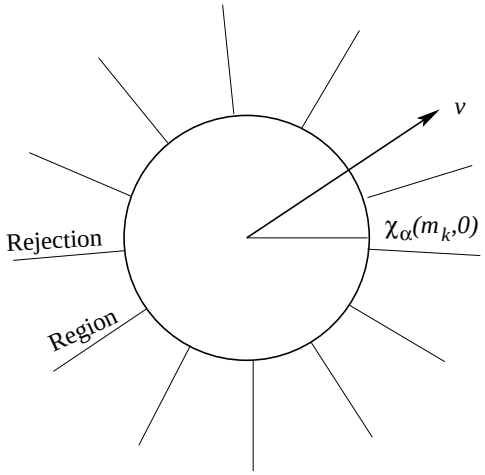

Fig. 4—Rejection region $T_{LOM}^k \geq F_\alpha(m_k, \infty, 0)$

3.2 Global Detection

The LOM-test discussed above may turn out to be too insensitive to global unmodelled trends in the mathematical model. Model errors that slowly build up as time proceeds may for instance have a high probability of passing the local detector unnoticed. This implies that the detection of global model errors requires test statistics with built in memory capabilities. Consider therefore the following two *global* hypotheses

$$H_0^{l,k} : \upsilon \sim \mathrm{N}(0, Q_\upsilon) \text{ vs } H_a^{l,k} : \upsilon \sim \mathrm{N}(C_\upsilon\nabla, Q_\upsilon) \quad (25)$$

with the vector of predicted residuals defined as

$$\upsilon = (\upsilon_l^T, \upsilon_{l+1}^T, ..., \upsilon_k^T)^T. \quad (26)$$

Note that the two hypotheses $H_0^{l,k}$, $H_a^{l,k}$ cover the time span [*l, k*]. In order to test the *overall* validity of the global hypothesis $H_0^{l,k}$, the mean $\nabla\upsilon = C_\upsilon\nabla$ of υ under $H_0^{l,k}$ should remain unspecified, which implies that matrix C_υ should be chosen as a square and regular matrix. By restricting T of (12) to the time interval [*l*, *k*], the invertible matrix C_υ gets eliminated and the appropriate UMPI-test statistic follows because of the block diagonal structure of Q_υ as

$$T^{l,k} = \sum_{i=l}^{k} \upsilon_i^T Q_{\upsilon_i}^{-1} \upsilon_i. \quad (27)$$

Note that $T^{l,k}$ reduces to (21) for the case *l*=*k*. After a normalization for the degrees of freedom, our global overall model test statistic can be formulated in the following *recursive* filter form:

$$\boxed{T_{GOM}^{l,k} = T_{GOM}^{l,k-1} + [\sum_{i=l}^{k} m_i]^{-1} \left[T^k - m_k \underline{T}_{GOM}^{l,k-1} \right]} \quad (28)$$

It is initialized by $T_{GOM}^{l,l} = T^l / m_l$. The UMPI-test statistic, $T_{GOM}^{l,k}$ is now used to perform a global overall model test for *detecting* unspecified model errors in the global hypothesis, $H_0^{l,k}$. The *global overall model* (GOM) test reads therefore as follows: An unspecified global model error is considered present in the time interval [*l*, *k*] if and only if

$$T_{GOM}^{l,k} \geq F_\alpha(\sum_{i=l}^{k} m_i, \infty, 0) \quad (29)$$

An important practical problem with the above GOM-test is the choice of *l*, the time that the model error is assumed to be starting to occur. Since the starting time of the model error is unknown *a priori* one has to start in principle with *l*=1. A fixed value of *l*, however, turns the filter (28) into a *growing-memory* filter, with the practical problem of a possible long delay in time of detection. Rejection of $H_0^{1,k}$ at time *k* with the GOM-test may imply namely that a global model error started to occur as early as time *l*=1. In order to reduce the time of delay, it is worthwhile to consider introducing a moving *window* of length *N* by constraining *l* to $k - N + 1 \leq l \leq k$. When choosing *N* one of course has to make sure that the detection power of the test is still sufficient. This is a typical problem one should take into consideration when designing a filter. With the finite window of length *N*, the filter (29) is essentially reduced to a *finite-memory* filter. Instead of using a finite window, one could also consider using a fading window. By setting *l* equal to 1 and replacing the gain $1/[\sum_{i=l}^{k} m_i]$ in (29) by the gain $w^k/[\sum_{i=l}^{k} m_i w^i]$, with $w \geq 1$, the filter reduces to a *fading-memory* filter. This has the advantage that the same recursive filter structure is retained. The value of *w*, which determines the length of the fading window, is chosen on the basis of the detection power of the test. Note that with the fading window we still have $\mathrm{E}\{T_{GOM}^{l,k} \mid H_0^{l,k}\} = 1$. But instead of following an *F*-distribution, the GOM-test statistic follows now a linear combination of independent χ^2-distributions.

4. IDENTIFICATION

4.1 Local Identification

The next step after detection is the identification of the most likely alternative hypothesis. As with detection, identification is based on the test statistic (12). For identification, however, candidate alternative hypotheses need to be specified explicitly. This specification is non-trivial and probably the most difficult task in the process of quality control. It depends to a great extent on experience and one's knowledge of the navigation system. For the present discussion we restrict attention to model errors in the measurement model. The theory is, however, also applicable for the case of model errors in the dynamic model [8]. The following class of local alternative hypotheses is considered

$$H_a^k : y_k = A_k x_k + C_k \nabla + e_k \quad (30)$$

This class of alternative hypotheses can be seen to model a *slip in the mean* of the vector of observables at time *k*. As such it can accommodate instrumental biases, sensor failures, and one or more outliers in the data. It is therefore particularly suited for the integrity monitoring of GPS-data. The dimension of the *b*-vector ∇ in (30) depends on the alternative hypothesis considered and can range for identification purposes from 1 to m_k. In case of outlier-identification, *b* equals the number of assumed outliers. We will first consider the case *b* = 1, that is, the case of a single model error.

4.1.1 Single Model Error

Since the local alternative hypothesis H_a^k of (30) is restricted to the measurement model, we have $C_{\upsilon_k} := C_k$. With *b* = 1, the vector ∇ reduces to a scalar and the matrix C_k reduces to a vector, which will be denoted by the lower case kernel letter c_k. By restricting T of (12) to

time k and taking the square-root, the test statistic takes the form

$$t^k = \frac{c_k^T Q_{\upsilon_k}^{-1} \upsilon_k}{\sqrt{c_k^T Q_{\upsilon_k}^{-1} c_k}} \tag{31}$$

This is the *local slippage* (LS) test statistic for the identification of a single local model error. Identification proceeds now as follows: The test statistic t^k is computed for each of the candidate one-dimensional alternative hypotheses. The alternative hypothesis for which the absolute value $|t^k|$ is at a maximum is then considered the one that contains the most likely model error. This is shown geometrically in Figure 5 for the two hypotheses, $c_{1,k}$ and $c_{2,k}$.

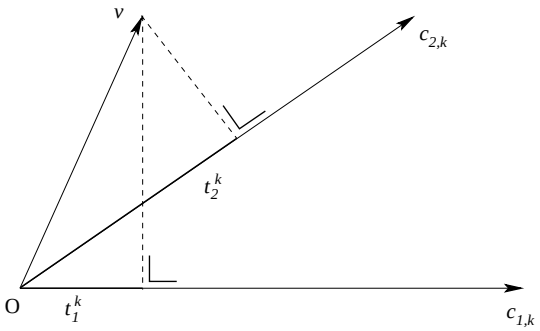

Fig. 5 — Two test statistics with $|t_2^k| > |t_1^k|$.

In the case of single outlier identification, the test statistic t^k is computed m_k-times, each time with a c_k-vector of the form $(0\ldots010\ldots0)^T$, with the 1 corresponding to the suspect observation. Once the most likely model error has been found, its likelihood needs to be tested. Since t^k is distributed under H_0^k and H_a^k as

$$H_0^k : t^k \sim \mathrm{N}(0,1) \text{ and } H_a^k : t^k \sim \mathrm{N}(\nabla[c_k^T Q_{\upsilon_k}^{-1} c_k]^{1/2}, 1) \tag{32}$$

the likelihood of the most likely model error can be tested by comparing $|t^k|$ with the critical value $\mathrm{N}_{\alpha_0/2}(0,1)$. If $|t^k| \geq \mathrm{N}_{\alpha_0/2}(0,1)$, then the corresponding most likely model error can be considered likely enough to have occurred. If however, the inequality $|t^k| < \mathrm{N}_{\alpha_0/2}(0,1)$ holds and the LOM-test diagnoses an unspecified model error, then one should reconsider the aptitude of the specified class of alternative hypotheses.

In a similar manner as (24) was proven, one can show that

$$\boxed{\lim_{P_{k|k-1}\to\infty} t^k = \frac{c_k^T R_k^{-1} \hat{e}_k}{\sqrt{c_k^T R_k^{-1} Q_{\hat{e}} R_k^{-1} c_k}}} \tag{33}$$

where $Q_{\hat{e}_k}$ is the variance matrix of the least-squares residual vector $\hat{e}_k$. For the special case that R_k is a diagonal matrix and the vector c_k has the canonical form $(0..010..0)^T$ with the 1 in the i^{th} place, (33) simplifies to $\lim_{P_{k|k-1}\to\infty} t^k = \hat{e}_{i,k} / \sigma_{\hat{e}_{i,k}}$. This test statistic is well known in geodesy and surveying, and usually forms the basis for the identification of outliers in geodetic networks [1-6]. In [9] the test statistic, $\hat{e}_{i,k}^2 / \sigma_{\hat{e}_{i,k}}^2$ has been derived for the case $R_k = \sigma^2 \mathrm{I}_{m_k}$.

4.1.2 Multiple Model Errors

As was pointed out earlier, the dimension of the b-vector ∇ in (30) depends on the alternative hypothesis considered and can range for identification purposes from 1 to m_k. In some applications the nature of the alternative hypothesis can be such that b is known. For instances, it may be known in a particular application that a sensor bias requires b number of additional parameters to model it. If b is known, one can follow in principle the same procedure as the one followed for the case of a single model error. The main difference is that the one-dimensional test statistic t^k needs to be replaced by its b-dimensional counterpart, which again is based on the UMPI-test statistic T of (12). If b is unknown, however, an alternative procedure needs to be developed. In this case one is faced with an *unknown* column dimension of the m_k-by-b matrix $C_{\upsilon_k} := C_k$. One approach of solving the problem is to start with a matrix C_k of which it is known that it describes all possible model errors. Then each of the columns of this matrix is considered separately and their corresponding test statistics t^k are computed. The b-number of model errors are then finally identified as those for which the sample of the corresponding test statistics $|t^k|$ exceeds the critical value $\mathrm{N}_{\alpha_0/2}(0,1)$. Experience has shown that this simple approach works well if *masking* is absent or at least minimal. The presence of masking, however, where for instance one model error may mask other model errors, introduces additional complications. In order to undo the masking, the idea is to remove, step by step, the most likely model errors and test after each step the likelihood of the remaining model errors. In this way one can at least guarantee that the likelihood test of the remaining model errors is free from the possible masking of the previously

removed most likely model errors. The procedure goes as follows: one starts as before with a matrix C_k of which it is known that it describes all possible model errors. Let us assume for simplicity that the full rank matrix C_k has the maximum allowable column dimension of m_k. The columns of the matrix C_k are denoted as c_i, $i = 1, \ldots, m_k$. In the first step one computes the test statistic

$$t_i^k = \frac{c_i^T Q_{\upsilon_k}^{-1} \upsilon_k}{\sqrt{c_i^T Q_{\upsilon_k}^{-1} c_i}}, \qquad (34)$$

for $i = 1, \ldots, m_k$, and identifies from this set the most likely model error, say j. This model error is then removed from the dataset by accounting for it in the measurement model. This results in an updated predicted residual with least-squares residual vector, $\hat{e}_{\upsilon_k(j)}$. This least-squares residual vector is then used for the detection of possible remaining model errors. This is done by means of the updated LOM-test,

$$T_{(j)}^k = \hat{e}_{\upsilon_k(j)}^T Q_{\upsilon_k}^{-1} \hat{e}_{\upsilon_k(j)} / (m_k - 1) \geq F_\alpha(m_\kappa - 1, \infty, 0) \qquad (35)$$

If this test is passed, the procedure is stopped and one model error, namely j, is considered to be identified. If the test fails, more than one model error is assumed to be present and the procedure continues with the second step of identification. In this second step, one computes the LS-test statistic

$$t_{i(j)}^k = \frac{c_i^T Q_{\upsilon_k}^{-1} \hat{e}_{\upsilon_k(j)}}{\sqrt{c_i^T Q_{\upsilon_k}^{-1} Q_{\hat{e}_{\upsilon_k(j)}} Q_{\upsilon_k}^{-1} c_i}}, \qquad (36)$$

for $i = 1, .., (j-1), (j+1), \ldots, m_k$ and identifies from this set the most likely model error. After removing this model error from the dataset the whole cycle of detection and identification is repeated again, until finally no model errors are detected. Although the procedure described above can be executed as such, it has in the form stated the computational disadvantage that it requires the explicit updating of $\hat{e}_{\upsilon_k(j)}$ and its variance matrix. Fortunately one can avoid the explicit updating of $\hat{e}_{\upsilon_k(j)}$ and its variance matrix if one interprets the above stepwise procedure as a recursive filter that operates in a *backward* mode. Instead of stepwise adding new information, one subtracts spurious information in a stepwise manner. This implies that the LOM-test statistic (35) can be formulated directly in the filter form

$$T_{(j)}^k = T^k - [m_k - 1]^{-1}[(t_j^k)^2 - T^k] \ , \qquad (37)$$

where $T^k = \upsilon_k^T Q_{\upsilon_k}^{-1} \upsilon_k / m_k$. Compare the structure of (37) with that of (28) and note the minus sign in the gain of (37) which is due to the backward recursion. Also the LS-test statistic (36) can be computed in recursive form. This result is based on the observation that $\hat{e}_{\upsilon_k(j)}$ is the orthogonal projection of υ_k onto the orthogonal complement of c_j. Thus we may write instead of (36),

$$t_{i(j)}^k = \frac{c_{i(j)}^T Q_{\upsilon_k}^{-1} \upsilon_k}{\sqrt{c_{i(j)}^T Q_{\upsilon_k}^{-1} c_{i(j)}}}, \qquad (38)$$

with

$$c_{i(j)} = P_{c_j}^{\perp} c_i \text{ and } P_{c_j}^{\perp} = [I - c_j [c_j^T Q_{\upsilon_k}^{-1} c_j]^{-1} c_j^T Q_{\upsilon_k}^{-1}] \qquad (39)$$

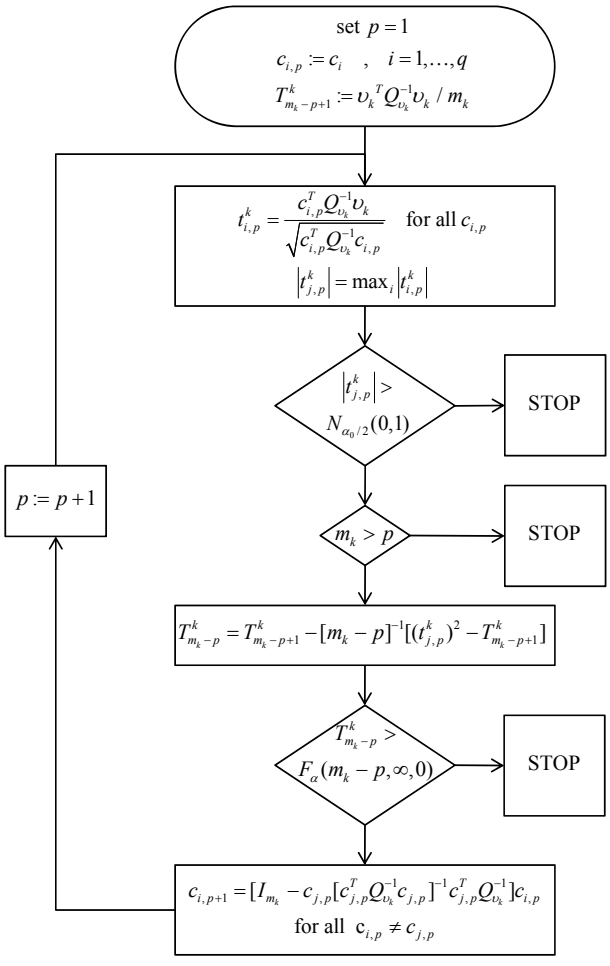

Fig. 6—Recursive local detection and identification of multiple model errors.

With (37) and (38) we are now in the position to solve the problem of local detection and identification of multiple model errors in a *recursive* form. This is shown in the flow diagram of Figure 6.

The likelihood test, $|t^k_{j,p}| \geq \mathrm{N}_{\alpha_0/2}(0,1)$, in Figure 6 is optional. It should be included, however, if model errors other than the ones described by c_i are considered present.

4.2 Global Identification

In order to identify global model errors that have been detected at time k for the time interval [l, k], alternative hypotheses need to be specified explicitly. Again attention is restricted to model errors in the measurement model. The following class of alternative hypotheses is considered

$$H_a^{l,k}: \; y_i = A_i x_i + C_i \nabla + e_i, \quad i = l, \cdots, k. \tag{40}$$

The matrices C_i of (40) propagate into the matrices C_{υ_i} of $C_\upsilon = (C^T_{\upsilon_l}, ..., C^T_{\upsilon_k})^T$ in (12) as

$$\begin{cases} C_{\upsilon_i} = C_i - A_i X_{i,l} \;, & i = l, ..., k \\ X_{i+1,l} = \Phi_{i+1,i}[X_{i,l} + K_i C_{\upsilon_i}] \;, & X_{l,l} = 0 \end{cases} \tag{41}$$

This propagation is recursive and corresponds of course with the propagation of the navigation filter itself. For convenience we will assume that ∇ is a scalar and C_i a vector. This restriction is, however, not essential. The discussion following is therefore in principle also applicable to the more dimensional case. For b = 1, we use the lower case kernel letter c_i, instead of C_i, and obtain - because of the block diagonal structure of Q_υ - from restricting the square root of T of (12) to the time interval [l, k], the test statistic

$$t^{l,k} = \frac{\sum_{i=l}^{k} c^T_{\upsilon_i} Q^{-1}_{\upsilon_i} \upsilon_i}{\sqrt{\sum_{i=l}^{k} c^T_{\upsilon_i} Q^{-1}_{\upsilon_i} c_{\upsilon_i}}} \tag{42}$$

This is the *global slippage* test statistic for the identification of a global one-dimensional model error. Strictly speaking, the test statistic, $t^{l,k}$ has to be computed for each alternative hypothesis considered and for each $k \geq l$. Moreover, since l, the time that the model error starts to occur, is unknown *a priori*, one has to start in principle with l = 1. This implies that one has to compute k number of test statistics, $t^{l,k}$, per alternative hypothesis at the time of testing k. As a result, one obtains a growing bank of global slippage test statistics. Clearly, this is unpractical, both from a computational point of view as well as because of the possible increase of the delay in time of identification. Fortunately, the growing bank of test statistics may not be necessary if one studies the *power* of the test statistics. Although the power will increase theoretically for an increasing size of the interval [l, k], the gain could be negligible for all practical purposes. This motivates, in accordance with our discussion of the global detection problem, the use of a moving window. By constraining l to $k - N + 1 \leq l \leq k$, a moving window of length N is introduced. The choice of N depends of course on the power required of the test statistic. Instead of constraining l to $k - N + 1 \leq l \leq k$, one may achieve some further computational savings by constraining l to $k - N + 1 \leq l \leq k - M$. The rationale behind this constraint is that in some applications the test statistic may be too insensitive for global model errors if $l > k - M$. Instead of using a finite window, the idea of a fading window as discussed in section 3.2 may be applied to the test statistic of (42) as well. The distribution of the test statistic will then follow under H_o a linear combination of independent χ^2-distributions, each with one degree of freedom. With the window introduced, we can now describe our identification procedure as follows: At the time of testing, k, one first determines per alternative hypothesis the value of l in the window for which the sample value of $|t^{l,k}|$ is at a maximum. This value of l, would then be the most likely time of occurrence of the model error if the corresponding alternative hypothesis would be true. In order to find both the most likely alternative hypothesis and most likely value of l, the sample values of $\max_{k-\mathrm{N}+1 \leq l \leq k-\mathrm{M}} |t^{l,k}|$ for the different alternative hypotheses are compared. The maximum of this set identifies then both the most likely time of occurrence l and the most likely alternative hypothesis. Since $t^{l,k}$ has a standard normal distribution under $H_0^{l,k}$, the likelihood of the corresponding alternative hypothesis can be tested by comparing the sample value of $t^{l,k}$ with the critical value $\mathrm{N}_{\alpha_0/2}(0,1)$. If it exceeds the critical value, the corresponding most likely alternative hypothesis can be considered likely enough to have occurred. Otherwise, one should consider the presence of model errors not belonging to the class as described by (40).

5. ADAPTATION

After identification of the most likely alternative hypothesis, adaptation of the recursive navigation filter is needed to eliminate the presence of biases in the filtered state of the navigation system. In order to be able to adapt the filter we first need an estimate of the identified model error ∇. The *best linear unbiased estimator* (BLUE) of

the b-vector ∇ under $H_a^{l,k}$ can be computed directly from the predicted residuals and it reads in its batch form as

$$\hat{\nabla}^{l,k} = [\sum_{i=l}^{k} C_{\upsilon_i}^T Q_{\upsilon_i}^{-1} C_{\upsilon_i}]^{-1} [\sum_{i=l}^{k} C_{\upsilon_i}^T Q_{\upsilon_i}^{-1} \upsilon_i]. \qquad (43)$$

In case of local identification we have $l = k$. The estimator of a single model error can then be computed directly from the LS-test statistic as $\hat{\nabla}^k = t^k / \sqrt{c_k^T Q_{\upsilon_k}^{-1} c_k}$. In case of multiple model errors we have $b \neq 1$, in which case the model error can be estimated as $\hat{\nabla}^k = [C_k^T Q_{\upsilon_k}^{-1} C_k]^{-1} [C_k^T Q_{\upsilon_k}^{-1} \underline{\upsilon}_k]$ where C_k is the matrix constructed from the vectors c_i that correspond with the identified model errors. If $l = k$, immediate corrective action is possible by resetting the navigation filter so that the adapted filtered state reads at time k,

$$\boxed{\hat{x}_{k|k}^a = \hat{x}_{k|k}^0 - K_k C_k \hat{\nabla}^k} \qquad (44)$$

where $\hat{x}_{k|k}^0$ and $\hat{x}_{k|k}^a$ are the filtered states corresponding with H_0 and H_a^k, respectively. The appropriate variance and covariance matrices follow from an error propagation of (44) as

$$\begin{cases} P_{k|k}^a &= P_{k|k}^0 + K_k C_k Q_{\hat{\nabla}^k} C_k^T K_k^T \\ P_{\hat{x}_{k|k}^a, \hat{\nabla}^k} &= -K_k C_k Q_{\hat{\nabla}^k}. \end{cases} \qquad (45)$$

The state vector $\hat{x}_{\kappa|\kappa}^{\alpha}$ and the variance matrix $P_{k|k}^a$ are then used for the new initialization at time k.

In the case of global identification we have $l \neq k$. Instead of using the batch form (43) it is now more expedient to use the following recursive filter form

$$\begin{cases} \hat{\nabla}^{l,k} &= \hat{\nabla}^{l,k-1} + G_k [\upsilon_k - C_{\upsilon_k} \hat{\nabla}^{l,k-1}] \\ Q_{\hat{\nabla}^{l,k}} &= [I - G_k C_{\upsilon_k}] Q_{\hat{\nabla}^{l,k-1}}, \end{cases} \qquad (46)$$

with gain matrix

$$G_k = Q_{\hat{\nabla}^{l,k-1}} C_{\upsilon_k}^T [Q_{\upsilon_k} + C_{\upsilon_k} Q_{\hat{\nabla}^{l,k-1}} C_{\upsilon_k}^T]^{-1}. \qquad (47)$$

This recursive filter is initialized with (43) for $k = l$. In the global case one is confronted with a delay in time of identification. This implies that in principle one has to correct the filtered states from time l to the present time k. This as a consequence would involve smoothing and may therefore be too heavy a computational burden. Instead the following simple approach is suggested. At time k, when the most likely alternative hypothesis has been identified, one resets the navigation filter by correcting the filtered state as

$$\boxed{\hat{x}_{k|k}^a = \hat{x}_{k|k}^0 - \Phi_{k,k+1} X_{k+1,l} \hat{\nabla}^{l,k}} \qquad (48)$$

where $\hat{x}_{k|k}^0$ and $\hat{x}_{k|k}^a$ are the filtered states corresponding with H_0 and $H_a^{l,k}$, respectively. An error propagation of (48) gives the variance and covariance matrices of the adapted state vector as

$$\begin{cases} P_{k|k}^a &= P_{k|k}^0 + \Phi_{k,k+1,} X_{k+l,l} Q_{\hat{\nabla}^{l,k}} X_{k+1,l}^T \Phi_{k,k+1}^T \\ P_{\hat{x}_{k|k}^a, \hat{\nabla}^{l,k}} &= -\Phi_{k,k+1} X_{k+1,l} Q_{\hat{\nabla}^{l,k}} \end{cases} \qquad (49)$$

Note that the n-by-b matrix $X_{k+1,l}$ can be computed recursively as shown in (41).

The above simple approach implies that the filtered states remain biased between times l and k. This bias may, however, be considered negligible if the build up of the global model error is still too small to be detected with the GOM-test statistic. This again points out that when designing the filter one should carefully consider the choice of window length and the detection power of the test in relation to the biases one is willing to accept. After the state vector has been corrected at time k for the model error, an adapted state vector, $\hat{x}_{k|k}^a$, is obtained which is free from bias. The question is now how to proceed from time k onwards. One could take $\hat{x}_{k|k}^a$ with its variance matrix as the new initial state and proceed as before with filtering under H_0. This has the advantage that the filter needs to be adapted only once and that the same navigation filter can be used. The disadvantage is, however, that this approach is only correct if the model error is indeed absent from time k onwards. Since this is not likely to be the case for global model errors, one will consequently notice in the predicted residuals that the model error slowly builds up again. In order to remedy this situation one could think of using the computed estimate of the model error at time k, for correcting the predicted residuals from time k onwards. In this approach, $\hat{x}_{k|k}^a$ with its variance matrix is used as the new initial state and the original filter is used with $y_i - C_i \hat{\nabla}^{l,k}$ instead of y_i and with $R_i + C_i Q_{\hat{\nabla}^{l,k}} C_i^T$ instead of R_i for $i > k$. The problem with this approach is, however, that it neglects the existing correlation between $\hat{x}_{k|k}^a$ and $\hat{\nabla}^{l,k}$ (see (49)). It is therefore only acceptable if this correlation can be considered negligible. This may for instance be the

case if the precision of the estimator of the model error is such that $Q_{\hat{\nabla}^{l,k}}$ is small enough. Although the above approximate methods may be good enough for certain applications, the proper way to keep track of the global model error is of course to use (48) not only at the time of testing *k* but for the complete duration of the model error. Mathematically this is equivalent to switching from filtering under H_0 to filtering under $H_a^{l,i}$ for $i \geq k$. Explicit filtering under $H_a^{l,i}$ implies, however, an augmentation of the state vector with ∇ and a corresponding change in all system matrices. Expression (48) has the advantage that this augmentation is not needed explicitly and that the state vector filtering can based on the nominal model. Thus an explicit parallel bank of navigation filters, as discussed in [10], can be avoided with the above set up.

6. THE MINIMAL DETECTABLE BIAS (MDB)

Undetected model errors in H_0 generally influence the mathematical expectation of the state vector estimator $\hat{x}_{k|k}$. It is therefore of importance to know how particular misspecifications in H_0 manifest themselves as biases in the state vector or functions thereof. Knowledge of the impact of model errors can then be used to set acceptance criteria for the sizes of these model errors. This is of great importance for the design of an appropriate navigation filter (e.g., redundancy of sensors, sensor precision, sampling rate, geometry, dynamics) and for the design of a powerful enough testing procedure (e.g., probabilities of false alarm and missed detection, window length).

Before considering the impact of model errors, one should of course first make clear on what functions of the state vector the impact is studied. This depends very much on the particular application for which the navigation filter is designed and it may range from just one single function of the state vector to all *n* elements of the state vector. For instance, the impact on instrumental nuisance parameters may or may not be of interest, or one may particularly be interested in position but not in velocity, or, as is the case in some GPS applications [11], it is the horizontal solution which is of interest and not the pseudorange-bias. In all these cases one generally has a set of linear(ized) functions of the state vector that is of particular interest. If we assume that the functions are collected in the *r*-by-*n* matrix F^T, then it is the bias, $F^T\nabla\hat{x}_{k|k}$, in $F^T\hat{x}_{k|k}$ which is of interest. The bias $F^T\nabla\hat{x}_{k|k}$ can be computed rather straight-fowardly from the equations that define the navigation filter. Once $F^T\nabla\hat{x}_{k|k}$ is known its significance can be tested with the following *bias-to-noise ratio* (BNR)

$$\boxed{\lambda_{F^T\hat{x}_{k|k}} = \nabla\hat{x}_{k|k}^T F[F^T P_{k|k} F]^{-1} F^T \nabla\hat{x}_{k|k}} \qquad (50)$$

Note that this scalar measure is *invariant* against reparametrizations of the state vector. Using Cauchy-Schwarz' inequality, the scalar $\lambda_{F^T\hat{x}_{k|k}}$, can be shown to give an upper bound on the bias-to-noise ratio of an arbitrary linear(ized) function of $F^T\nabla\hat{x}_{k|k}$:

$$\boxed{\frac{(a^T F^T \nabla\hat{x}_{k|k})^2}{a^T (F^T P_{k|k} F) a} \leq \lambda_{F^T\hat{x}_{k|k}}, \forall a \in \mathbb{R}^r} \qquad (51)$$

This shows, for *F*=*I*, that $\lambda_{F^T\hat{x}_{k|k}}$ gives an upper bound for the bias-to-noise ratios of all the individual elements of the state vector $\hat{x}_{k|k}$.

Assuming that for a particular application a quantification of the demands is given in terms of criteria for $\lambda_{F^T\hat{x}_{k|k}}$, (50) can be used to determine the sizes of the model errors that should be detectable by the statistical tests at a certain level of probability. This brings us then to the important concept of the power of a statistical test. The power γ of a statistical test, being the probability of rejecting H_0 when an alternative hypothesis H_a is true, depends on the chosen level of significance α (probability of false alarm), the number of degrees of freedom *b*, and the non-centrality parameter λ, of the corresponding test statistic:

$$\gamma = \gamma(\alpha, b, \lambda). \qquad (52)$$

The power γ is a monotonic increasing function in α and λ, and a monotonic decreasing function in *b*. Since λ depends on the assumed model errors in H_0, the power function (52) can be used to determine how well particular model errors can be detected with the associated test. A low probability corresponds with poor detectability. Instead of using the power function (52), we propose to use the *inverse power function*

$$\lambda = \lambda(\alpha, b, \gamma). \qquad (53)$$

The rationale for using the "inverse power function" is that in practical applications one is usually much more interested in the size of the model error that can be detected with a certain probability γ, than in the power γ itself. If we assume that under the true hypothesis,

$$\mathrm{E}\{\upsilon \mid H_{true}\} = \bar{C}_\upsilon \nabla \quad , \qquad (54)$$

then the non-centrality parameter of the test statistic T becomes

$$\lambda = \nabla^T \bar{C}_\upsilon^T Q_\upsilon^{-1} C_\upsilon [C_\upsilon^T Q_\upsilon^{-1} C_\upsilon]^{-1} C_\upsilon^T Q_\upsilon^{-1} \bar{C}_\upsilon \nabla. \quad (55)$$

This may be written in geometric terms as

$$\lambda = \| P_{C_\upsilon} \bar{C}_\upsilon \nabla \|^2 = \| \bar{C}_\upsilon \nabla \|^2 \cos^2 \phi, \quad (56)$$

where ϕ is the angle between $\bar{C}_\upsilon \nabla$ and the range space of C_υ. The angle ϕ is therefore a measure of *separability* between H_a and H_{true}. It becomes more difficult to distinguish between the hypotheses H_a and H_{true} if ϕ decreases. If we assume that H_a and H_{true} only differ in their time of occurrence, then $\cos^2 \phi$ can be used as a *diagnostic tool* for inferring how well the true starting time of the model error can be determined. This was illustrated in [6]. With (53) and (55) we are now in the position to compute the hyper ellipsoidal boundary region of biases that can be detected with a chosen reference probability, γ_0, and introduce the concept of a *minimal detectable bias* (MDB). An MDB is defined as the model error, ∇, that can just be detected with the UMPI-test statistic of section 4. With the parametrization $\nabla = \| \nabla \| e$, $e \in \mathbb{R}^b$, where e is a unit vector, and $\lambda_0 = \lambda(\alpha, b, \gamma_0)$, the MDB follows from (56) as

$$\boxed{\nabla^{l,k} = e \sqrt{\frac{\lambda_0}{\| P_{C_\upsilon} \bar{C}_\upsilon e \|^2}}} \quad (57)$$

As the following examples show, the MDBs provide an important *diagnostic tool* for inferring how well particular model errors can be detected. With the MDBs we now also have a measure for the model errors that can be propagated in the *design phase* of the navigation filter (that is, when no actual measurements are available) to get $F^T \nabla \hat{x}_{k|k}$ which is needed for (50).

Example 1 [16]

Assume that H_a and H_{true} only differ in their time of occurrence l and l_o, respectively. Furthermore, assume that $b = 1$. Then (57) reduces to

$$| \nabla_{l_o}^{l,k} | = \sigma_{\hat{\nabla}^{l_o,k}} \sqrt{\frac{\lambda_0}{\sigma_{t^{l,k}, t^{l_o,k}}}} \quad (58)$$

where $\sigma_{t^{l,k}, t^{l_o,k}}$ is the covariance (or correlation coefficient) between the LS-test statistics, $t^{l,k}$ and $t^{l_o,k}$. The covariance $\sigma_{t^{l,k}, t^{l_0,k}}$ reaches its maximum of 1 for $l = l_0$. Hence, since $\sigma_{\hat{\nabla}^{l_0,k}}$ is independent of l, $| \nabla_{l_0}^{l,k} |$ has its minimum at $l = l_0$. This is of course in agreement with the fact that the test statistic is most powerful for $l = l_o$. The minimum of $| \nabla_{l_0}^{l,k} |$ decreases for increasing k. That is, when $l = l_0$, larger values of k correspond with biases of a smaller size that can be detected with a probability γ_o. This result can be used to make an appropriate choice for the window length N. For instance, if in a particular application a criterion is set at a level of probability γ_o for the size of the MDB, k and therefore N can be chosen such that $| \nabla_{l_o}^{l,k} |$ meets the criterion. In order to illustrate the characteristics of $| \nabla_{l_o}^{l,k} |$, we consider for the model parameters $\Phi_{k,k-1} = 1,\ A_k = 1,\ P_{0|0} = p,\ R_k = r, Q_k = 0$, the following two alternative hypotheses:

H_{a1}: An outlier in the data at time l_o

H_{a2}: A sensor failure that starts at time l_o.

The MDBs for these two alternative hypotheses read:

$$H_{a1}: \quad | \nabla_{l_0}^{l,k} | = \begin{cases} [\lambda_0\, r(r/p+k)(r/p+k-1)]^{1/2} \\ \text{for } l \neq l_0 \\ [\lambda_0 r(r/p+k)(r/p+k-1)^{-1}]^{1/2} \\ \text{for } l = l_0 \end{cases}$$

$$H_{a2}: | \nabla_{l_0}^{l,k} | = \begin{cases} \left[\lambda_0 \dfrac{r(r/p+k)}{(k-l+1)(r/p+l-1)}\right]^{1/2} \left[\dfrac{k-l+1}{k-l_0+1}\right] \\ \text{for } l \leq l_0 \\ \left[\lambda_0 \dfrac{r(r/p+k)}{(k-l+1)(r/p+l-1)}\right]^{1/2} \left[\dfrac{r/p+l-1}{r/p+l_0-1}\right] \\ \text{for } l \geq l_0 \end{cases}$$

In Figures 7 and 8 the ratio $| \nabla_{l_0}^{l,k} | / \sqrt{\lambda_0}$ is plotted as a function of l for different values of $k \geq l_0$. Figure 7 corresponds with hypothesis H_{a1}. Comparison of Figure 7a with 7b shows the influence of an increase in measurement precision on the size of the MDB.

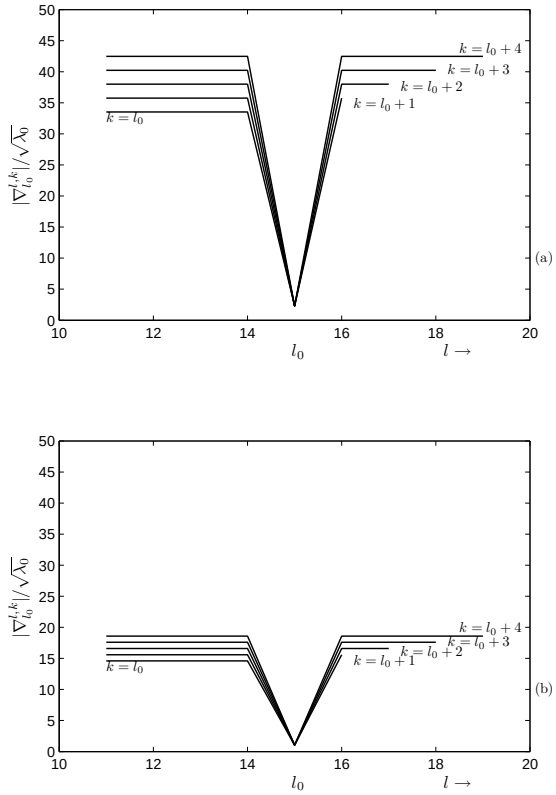

Fig. 7: $|\nabla^{l,k}_{l_0}|/\sqrt{\lambda_0}$ for outlier at l_o: (a) p = 10, r = 5, l_o = 15; (b) $p = 10$, $r = 1$, $l_o = 15$.

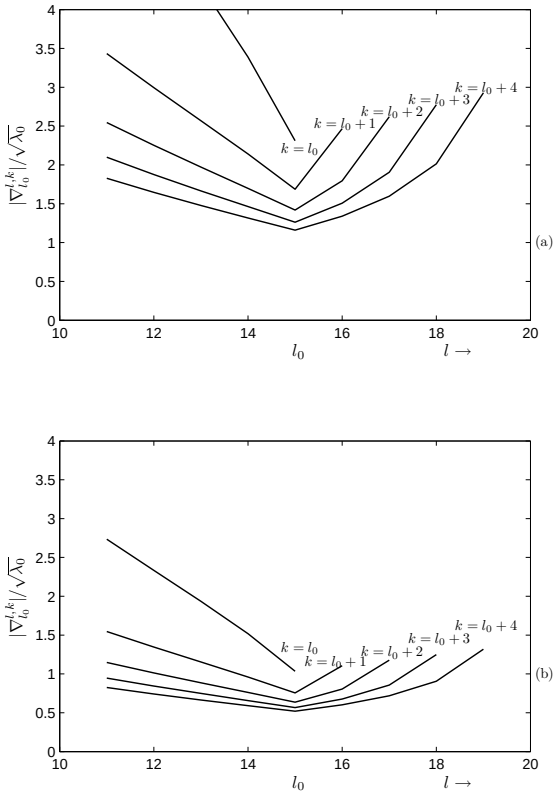

Fig. 8: $|\nabla^{l,k}_{l_0}|/\sqrt{\lambda_0}$ for slip at l_o: (a) $p = 10$, $r = 5$, $l_o = 15$; (b) $p = 10$, $r = 1$, $l_o = 15$.

Figure 7 also shows that the minimum of $|\nabla^{l,k}_{l_0}|$ at l_o gets more pronounced for increasing k. This is characteristic of local model errors and shows that it becomes easier to determine the correct time of occurrence, l_o, of an outlier when k increases.

Figure 8 corresponds with hypothesis H_{a2}. In this figure $|\nabla^{l,k}_{l_0}|/\sqrt{\lambda_0}$ is plotted for two different values of r. The figure shows that $|\nabla^{l,k}_{l_0}|$ decreases for $l < l_o$ that it obtains its minimum at $l = l_o$, and that it increases at a somewhat faster rate for $l < l_o$. The figure also shows the decrease in the minimum for increasing k. But note, since

$$\lim_{k\to\infty} |\nabla^{l,k}_{l_0}| = \begin{cases} \left[\lambda_0 \dfrac{r}{r/p + l - 1}\right]^{1/2} \\ \text{for } l \le l_0 \\ \left[\lambda_0 \dfrac{r}{r/p + l - 1}\right]^{1/2} \left[\dfrac{r/p + l - 1}{r/p + l_0 - 1}\right] \\ \text{for } l \ge l_0 \end{cases}$$

that the improvement in the MDB is not without bounds. Hence, it does not pay to test with $t^{l_0,k}$ after a certain time delay. Comparison of Figure 8a with 8b shows the influence of an increase in measurement precision on the size of the MDB. The gradient with respect to k of $|\nabla^{l,k}_{l_0}|$ at $l = l_o$ increases, and the minimum of $|\nabla^{l,k}_{l_0}|$ decreases for decreasing r.

Example 2 [14]

In this example the navigation of a vessel in the North Sea is considered. The North Sea area is a good example of a region where integration can be considered as it is covered by various radio positioning systems. It is chosen to oppose a non-integrated solution with an integrated solution. The non-integrated solution is based on the Syledis-system in range-range mode, where up to four uncorrelated ranges are used with a variance of 2.25 m^2 for the positioning of the vessel. The measurement interval is one second and the vessel is sailing a straight course at 5 m/s. The dynamic model is based on a constant velocity model with the acceleration noise having a variance of 0.0625 m^2/s^4. The four Syledis transmitters are evenly distributed around the vessel's position and provide for good coverage. Figure 9 shows some typical MDBs corresponding with outliers in the Syledis-ranges, sensor failure of Syledis-channels, and slips in position and velocity due to an unmodelled acceleration along and across track. The level of significance, $\alpha_\circ$, and power, $\gamma_\circ$, were chosen as $\alpha_\circ = 0.001$ and $\gamma_\circ = 0.80$.

H_a's related to observations			
H_a type	outlier		slip
delay	(0)	(4)	(4)
Syledis 1[m]	6.95	6.45	3.43
Syledis 2[m]	7.44	6.56	4.17

H_a's related to slip in state vector		
H_a type	slip	
delay	(1)	(4)
acc. along track [m/s^2]	3.46	0.828
acc. across track [m/s^2]	3.68	0.861

Fig. 9—MDBs with Syledis as stand-alone system.

Syledis 1 and Syledis 2 in Figure 9 refer to the best and worst MDBs for the four ranges. The differences are fairly small, which is due to the good Syledis geometry. Note that with increasing delay the MDB improves considerably for an H_a related to a slip in the observations and an unmodeled acceleration, but hardly for an H_a related to an outlier. This indicates that the slippage tests related to the first two H_a's require a considerable larger window length than the tests related to outliers in the observations.

In the integrated solution, Syledis is integrated with Hifix/6, a gyro compass and a log in bottom track mode. Two Hifix/6 hyperbolic lines of position (lops) are used with a variance of $6m^2$ and a correlation of 1.6 m^2 between lops. The gyro has a variance of 0.0625 deg^2 and the log a variance of 0.04 m^2/s^2. The dynamic model is augmented with a gyro drift and log bias. The gyro drift system noise is modeled as a drift rate of 0.0025 deg^2/s^2 and the log bias system noise is modeled as a drift rate of 0.0001 m^2/s^2. Figure 10 shows some typical MDBs for the integrated solution.

H_a's related to observations			
H_a type	outlier		slip
delay	(0)	(4)	(4)
Syledis [m] (worst)	6.57	6.39	3.47
Hifix [m] (worst)	9.90	9.84	4.61
gyro [deg]	12.10	8.50	7.80
log [m/s]	1.46	1.16	0.86

H_a's related to slips in state vector		
H_a type	slip	
delay	(1)	(4)
acc. along track [m/s^2]	0.904	0.502
acc. across track [m/s^2]	0.741	0.465
gyro drift [deg]	8.1	3.1
log bias [m/s]	0.84	0.31

Fig. 10—MDBs with Syledis, Hifix/6, gyro and log integrated.

In the integrated solution, the MDBs of the Syledis ranges improve somewhat but not considerably. This is due to the good Syledis coverage. A mayor improvement is seen, however, in the MDBs related to the H_a concerning a slip caused by an unmodeled acceleration. Also note that in contrast with Syledis and Hifix, the MDBs for an outlier of gyro and log do improve with increasing window length.

ACKNOWLEDGEMENT

The expert type-setting by Miriam Lewis from the Institute of Navigation (ION) is greatly appreciated. The original 1990-text was type-set in LaTex by J. Blotwijk.

7. REFERENCES

1. Mierlo, J. van, "Statistical Analysis of Geodetic Networks Designed for the Detection of Crustal Movements," *Progress in Geodynamics*, Borrodaile, G. J., et al. (Eds.), North-Holland Publishing Company, pp. 45-51.
2. Kok, J. J., "Statistical Analysis of Deformation Problems using Baarda's Testing Procedure," *Forty Years of Throught,* Delft, 1982 Vol. 2, pp. 470-488.
3. Baarda, W., "A Testing Procedure for Use in Geodetic Networks," *Netherlands Geodetic Commission*, Publications on Geodesy, New Series, 1968, Vol. 2, No. 5, Delft.
4. Teunissen, P. J. G., "Quality Control in Geodetic Networks," *Optimization and Design of Geodetic Networks*, Grafarend, E. and Sanso, F. (Eds.), Springer Verlag, Berlin, 1984, pp. 526-547.

5. Teunissen, P. J. G., “Adjusting and Testing with the Models of the Affine and Similarity Transformation,” *Manuscripta Geodaetica*, 1986, Vol. 11, pp. 214-225.
6. Förstner, W., “Results of Test I on Gross Error Detection of ISP WG III/1 and OEEPE,” ISP Comm. III, 1982 Helsinki.
7. Staff of DGCC, “The Delft Approach of the Design and Computation of Geodetic Networks,” *Forty Years of Thought*, Delft, 1982, Vol. 2, pp. 202-274.
8. Parkinson, B. W., and Axelrad P., “Autonomous GPS integrity Monitoring Using the Pseudorange Residual,” *NAVIGATION*, Vol. 35, No. 2, 1988, pp. 255-274.
9. Sturza, M. A., “Navigation Systems Integrity Monitoring Using Redundant Measurements,” *NAVIGATION*, Vol. 35, No. 4, 1988, pp. 483-501.
10. Brown, G. and Hwang, P. Y. C., “GPS Failure Detection by Autonomous Means within the Cockpit,” *NAVIGATION*, Vol. 33, No. 4, 1987, pp. 335-353.
11. Brown, R. G., and McBurney, P. W., “Self-Contained GPS Integrity Check Using Maximum Solution Separation,” *NAVIGATION*, Vol. 35, No. 1, 1988, pp. 41-53.
12. Teunissen, P. J. G., and Salzmann, M. A., “Performance Analysis of Kalman Filters,” *Proceedings of HYDRO 88*, Special Publications, No. 23, Hydrographic Society, 1988, pp. 185-193.
13. Enge, P. K., Vicksell, F. B., Goodard, R. B., and van Graas, F., “Combining Pseudoranges from GPS and Loran-C for Air Navigation,” *NAVIGATION*, Vol. 37, No. 1, 1990, pp. 95-112.
14. Salzmann, M. A., “MDB: A Design Tool for Integrated Navigation Systems,” *Int. Symposium on Kinematic Systems in Geodesy, Surveying and Remote Sensing*, Banff, Canada, 1990.
15. Teunissen, P. J. G., and Salzmann, M. A., “A Recursive Slippage Test for Use in State-Space Filtering, ” *Manuscripta Geodaetica*, Vol. 14, No. 6, 1989, pp. 383-390.
16. Teunissen, P. J. G., “Quality Control in Integrated Navigation Systems,” *IEEE Aerospace and Electronic Systems Magazine*, Vol. 5, No. 7, 1990, pp. 35-41.